Correlation of local and global orientation and spatial frequency tuning in macaque V1

Dajun Xing[1], Dario L. Ringach[2], Robert Shapley[1] and Michael J. Hawken[1]

[1] *Center for Neural Science, New York University, New York, NY 10003, USA*
[2] *Departments of Neurobiology, Psychology, and, Brain Research Institute, University of California, Los Angeles, Los Angeles, CA 90095, USA*

Visual cortical neurones display a variety of visual properties. Among those that emerge in the primary visual cortex V1 are sharpening of selectivity for spatial frequency and for orientation. The selectivity for these stimulus attributes can be measured around the peak of the tuning function, usually as bandwidth. Other selectivity measures take into account the response across a broader range of stimulus values. An example of such a global measure is the circular variance of orientation tuning. Here we introduce a similar measure in the spatial frequency domain that takes into account the shape of the tuning curve at frequencies lower than the peak, called the low-spatial frequency variance. Our recent studies with dynamic stimuli suggest that the selectivity for spatial frequency and orientation is strongly correlated with the degree of suppression at low spatial frequencies and off-axis orientations. Here we extend the study of the global tuning to stimulus conditions that measure the response of cells to the presentation of drifting sinusoidal grating stimuli for periods of a few seconds. We find that under such steady-state stimulus conditions there is a strong correlation between the global selectivity measures, orientation circular variance and low spatial frequency variance. Consistent with previous studies, there is a weaker correlation between the local tuning measures, orientation and spatial frequency bandwidth. These results support the idea that there are multiple factors that contribute to tuning and that suppression observed in dynamic experiments is also likely to contribute to the global selectivity for steady-state stimuli.

(Received 30 January 2004; accepted after revision 16 April 2004; first published online 16 April 2004)
Corresponding author D. Xing: Center for Neural Science, New York University, New York, NY 10003, USA. Email: xdj@cns.nyu.edu

V1 neurones show a range of selectivity for stimulus orientation and spatial frequency. Broad tuning for spatial frequency is established first at the level of the retina by the centre–surround organization of receptive fields (Kuffler, 1953; Enroth-Cugell & Robson, 1966). This tuning is further refined at the level of the cortex where tuning becomes considerably narrower than it is in single neurones in the lateral geniculate nucleus LGN (Campbell *et al.* 1969; Movshon *et al.* 1978; DeValois *et al.* 1982) that provide the input to V1. Orientation tuning is mainly developed at the level of the cortex. One of the questions that has been at the forefront of recent experimental and theoretical investigations of cortical tuning is how much of the tuning is due to feed-forward mechanisms at the input to cortex and how much is due to intracortical mechanisms (Nelson *et al.* 1994; Ben-Yishai *et al.*, 1995; Reid & Alonso, 1995; Somers *et al.* 1995; Ferster *et al.* 1996; Troyer *et al.* 1998; Adorjan *et al.* 1999; McLaughlin *et al.* 2000; Bruno & Simons, 2002; Ringach *et al.* 2002*a*, 2003; Miller, 2003; Shapley *et al.* 2003).

Recently, we used dynamic stimuli to show that a cell's responses at spatial frequencies around and below optimal and orientations far from the peak were suppressed (Ringach *et al.* 2002*a*). Importantly, selectivity was correlated with the degree of suppression in orientation and spatial frequency. Since we showed there is a link between suppression in the orientation and spatial frequency domains and selectivity, we can predict a strong correlation between the sharpness of tuning in these two domains.

However, a previous study of the relationship between the selectivity for spatial frequency and orientation found only a moderate correlation when orientation and spatial frequency bandwidths were used as measures of selectivity (DeValois *et al.* 1982). One of the main differences between DeValois *et al.*'s study and our recent investigations

 DOI: 10.1113/jphysiol.2004.062026

(Ringach *et al.* 2002*a*) was that DeValois *et al.* used steady-state stimuli (drifting gratings presented for a few seconds) while Ringach *et al.* (2002*a*) used dynamic stimuli (flashed gratings presented for 20 ms). Our aim here was to use steady-state stimuli, similar to those used by DeValois *et al.* to study the interrelationship between spatial frequency and orientation selectivity. We also thought it was important to use and to compare different measures of selectivity from those used by DeValois *et al.* (1982).

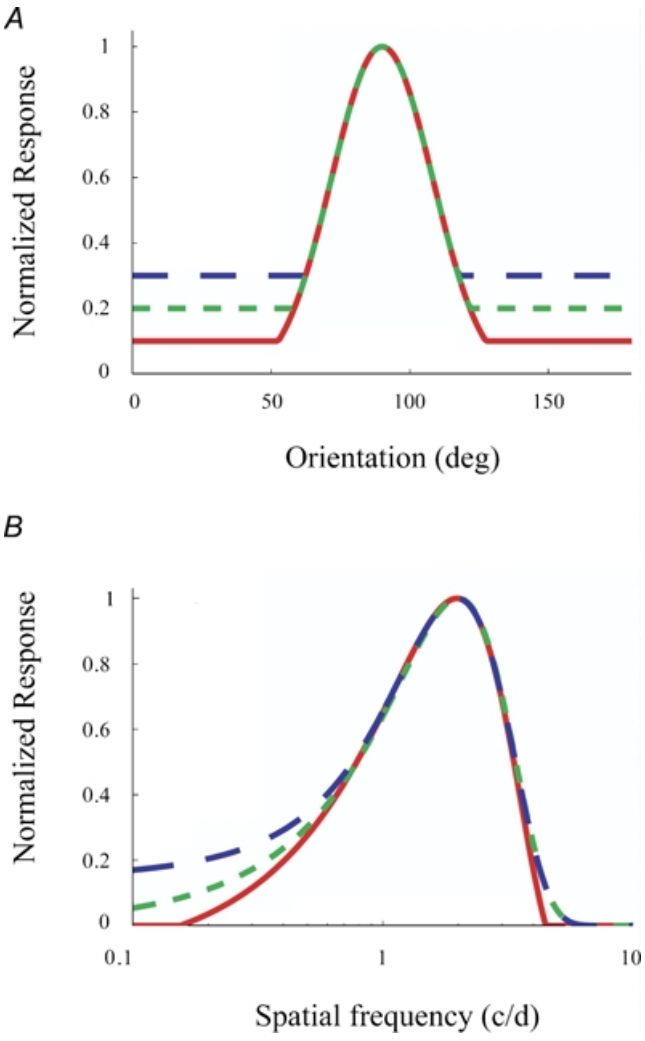

Figure 1. Hypothetical tuning curves
A, the tuning of three hypothetical orientation tuning curves. Each curve has the same orientation bandwidth (Ori_bw) but different degrees of attenuation near the orthogonal orientation, and hence each cell has a different orientation circular variance (Ori_CV). *B*, the tuning of three hypothetical spatial frequency tuning curves. Each curve has the same spatial frequency bandwidth (Sf_bw) but different degrees of attenuation at low spatial frequencies, and hence each cell has a different low spatial frequency variance (LSFV).

An examination of the different measures of selectivity makes it clear that they are based on different aspects of the response. It is possible that there are processes that set up the local tuning around the peak of the tuning function and different, more global processes that refine the tuning away from the peak. We can use different measures of selectivity to estimate the effects of different processes on orientation and spatial frequency selectivity. Earlier studies concentrated on measures that examined the bandwidths of orientation and spatial frequency tuning curves. The bandwidth measures the sharpness of tuning around the peak of the tuning function (Fig. 1). However, tuning functions can have the same bandwidth yet quite different responses well away from the peak as shown in the hypothetical tuning functions in Fig. 1 and also in the data (Fig. 3). One of the features of cortical responses is that the most highly selective cells are silent at orthogonal orientations and at spatial frequencies away from the peak. For high spatial frequencies the response attenuation is probably related to the smallest subunit size of the receptive field (Parker & Hawken, 1988). For low spatial frequencies a suppressive component has been demonstrated (Ringach *et al.* 2002*a*). A similar phenomenon is seen in the orientation domain. Cells with the same orientation bandwidth can have different circular variance (Ringach *et al.* 2002*b*) because low circular variance (high selectivity) appears to be caused by suppression of responses to orientations far from the peak.

Previous studies in primates reported a correlation coefficient of around 0.5 between orientation bandwidth and spatial frequency bandwidth (DeValois *et al.* 1982). This result tells us about the tuning around the peak spatial frequency and preferred orientation, the local tuning. Our new results presented below indicate that global tuning measured by orientation circular variance and that measured by low spatial frequency variance (a new global measure of spatial frequency selectivity introduced here) show a higher correlation, around 0.75. This result suggests that similar processes suppress off-peak orientation responses and low spatial frequency responses, and that these processes may be distinct from those that produce the tuning around the peak. These results have important implications for the classes of models of cortical circuitry that can be used to account for orientation and spatial frequency selectivity.

Methods

Preparation

Acute experiments of several days duration were performed on adult old-world monkeys (*Macaca*

fascicularis) in compliance with National Institutes of Health (NIH) and New York University (NYU) guidelines. Animal preparation and recording were done as previously described (Hawken *et al.* 1996; Ringach *et al.* 2002*b*). Animals were initially tranquilized with acepromazine (50 μg kg^{-1}). After the tranquilizer, the animal was anaesthetized by ketamine (30 mg kg^{-1}, I.M.) for venous cannulation and tracheotomy. Triple antibiotic ointment was applied surrounding the incisions. Additional ketamine was given during this surgery if needed. After cannulation and tracheotomy, the animal was placed in a stereotaxic frame for craniotomy and subsequent visual experiments. Further surgery was performed under sufentanyl (6–18 μg kg^{-1} h^{-1}, I.V.) anaesthesia. A craniotomy (5 mm or smaller in radius) was made in one hemisphere 4 mm posterior to the lunate sulcus (15–20 mm anterior to the occipital ridge) and 15 mm lateral to the mid line. Then the dura was cut (less than 1 mm in radius) to provide access for the electrode. During the whole duration of the acute experiment, anaesthesia was continued with sufentanyl (6–18 μg kg^{-1} h^{-1}, I.V.) and the animal was neuromuscularly blocked with pancuronium bromide (0.1 mg kg^{-1} h^{-1}, I.V.). Anaesthetic state was monitored by maintaining a slow wave EEG activity pattern and tested so that potentially mildly noxious stimuli produced no change in EEG, heart rate, or blood pressure. Expired CO_2 was maintained close to 5%. Temperature was kept at a constant 37°C. A broad spectrum antibiotic (Bicillin, 50 000 IU kg^{-1}, I.M.) and anti-inflammatory steroid (dexamethasone, 0.5 mg kg^{-1}, I.M.) were given on the first day of the experiment and on alternate days during the recording period. Experiments were terminated with a lethal dose of pentobarbital (60 mg kg^{-1}, I.V.).

Ophthalmic atropine sulphate (1%) was initially administered to the eyes in order to dilate the pupils. A topical antibiotic solution (gentamicin sulphate, 3%) was then applied to the eyes. For the duration of the experiment, the eyes were protected by clear, gas-permeable contact lenses and were inspected frequently during the experiment to ensure that the optics were clear. The foveae were mapped onto a tangential screen using a reversing ophthalmoscope. The visual receptive fields of isolated single neurones were then mapped onto the tangent screen with reference to the foveae.

Recording

Extracellular recording. We recorded single units with a glass-coated tungsten microelectrode (5–10 μm tip size). The electrode advanced through the cortex via a stepping motor (1 μm step size) mounted to a Narashige microdrive. The electrical signal was amplified using a Dagan EX4-400 differential amplifier (Dagan Corp. Minneapolis, MN, USA) and band-pass filtered (0.1–10 kHz). In earlier experiments, impulses triggered by each action potential were detected with a Bak dual window discriminator (Bak Electronics, Mount Airy, MD, USA) and were time-stamped with 1 ms precision and stored by a CED-1401+ data acquisition system (Cambridge Electronic Design, Cambridge, UK). In more recent experiments, spikes were discriminated and time-stamped with 1 ms accuracy by means of custom-designed software running on a Silicon Graphics O2 computer. Strict criteria for single-unit recording were used, including fixed shape of the action potential and absence of spikes during the absolute refractory period.

The visual stimuli were generated on a Silicon Graphics O2 R5000 computer. Stimuli were displayed on a Sony Multiscan 17se II colour monitor (31.4 cm wide and 23.5 cm high) with a resolution of 800 × 600 pixels. The CRT refresh rate was 60 Hz for some of the earlier experiments and 100 Hz for experiments thereafter and its mean luminance was 53 cd m^{-2}. The viewing distance was 90–120 cm.

Each cell was stimulated monocularly through the dominant eye and characterized by measuring its steady-state response to conventional drifting gratings (the non-dominant eye was occluded). Drifting gratings were presented for 2–4 s, and steady-state response was the mean firing rate during this period. Using this method, we recorded basic attributes of the cell, including spatial and temporal frequency tuning, orientation tuning, contrast and colour sensitivity, as well as area summation curves. Receptive fields were located at eccentricities between 1 and 6 deg.

Spatial frequency and orientation tuning

As part of our general characterization of neurones we include spatial frequency and orientation tuning as basic experiments. In the present experiments, we measured tuning curves for steady-state stimuli, drifting gratings, which vary in orientation and spatial frequency. We have recently described procedures for measuring the orientation tuning to drifting grating stimuli and the methods for analysis of the tuning curves (Ringach *et al.* 2002*b*). Briefly, orientation was measured in steps of 20 deg or less for stimuli of the optimal spatial and temporal frequency. In the standard experiments contrast was usually 0.8 (though occasionally it was set to 0.64, with no obvious difference).

Spatial frequency tuning was determined in half-octave steps for a range of frequencies that covered the response range of each cell. For each cell a circular window was used to optimize the response of the cell. There were a number of cells that we obtained data for where the window did not include at least two cycles of the grating at the optimal spatial frequency. These cells are not included in the dataset shown here. Each tuning function was fitted with a difference of Gaussians to obtain a smoothed curve for calculating the spatial frequency bandwidth (Sceniak *et al.* 2001; Fig. 2 right column).

Orientation tuning bandwidth. Given a cell's orientation tuning curve, we smoothed the curve with a Hanning window filter whose length is 18 deg (Ringach *et al.* 2002*b*; Fig. 2 left column). Then we found the peak response in the smoothed curve, and looked for the points on both sides of the peak at which the cell's responses were just half of the peak response. Half of the distance between the two points is the orientation bandwidth. If there is no response smaller than half of the peak, then the cell is called not-orientated and its orientation tuning bandwidth is set to 180 deg.

$$\text{Ori\_bw} = \frac{\text{Ori}_{\text{high}} - \text{Ori}_{\text{low}}}{2} \tag{1}$$

Circular variance. Given a cell's orientation tuning curve, we usually have 18 different responses of the cell to different orientations over the range 0 to 360 deg usually with 20 deg intervals. We call them r_i ($i = 1, 2, \ldots 18$) for each orientation. The orientation circular variance was defined by the following function:

$$\text{Ori\_CV} = 1 - \frac{\left|\sum_{j=1}^{18} r_j e^{i2\theta_j}\right|}{\sum_{j=1}^{18} r_j} \tag{2}$$

In the spatial frequency-tuning experiment, we used drifting gratings with optimal orientation, temporal frequency, radius and high contrast to stimulate the cell's receptive field. Cells' responses were measured to 10 gratings of different spatial frequencies evenly distributed between 0.1 and 10 cycles deg^{-1} on a logarithmic scale. To characterize a cell's spatial frequency tuning, we fitted the data with a DOG (difference of Gaussians) model to minimize the square error between the DOG curve and real data, with all parameters (R_0, K_e, μ_e, σ_e, K_i, μ_i and σ_i) free:

$$R(\text{Sf}) = R_0 + K_e e^{\frac{-(\text{Sf}-\mu_e)^2}{2\sigma_e^2}} - K_i e^{\frac{-(\text{Sf}-\mu_i)^2}{2\sigma_i^2}} \tag{3}$$

Spatial frequency tuning bandwidth. Based on the fitted curve, we found the peak of the curve, and looked for the points where the curve dropped to half of the peak, denoted Sf_{high} and Sf_{low}. The spatial frequency bandwidth is defined in the following equation:

$$\text{Sf\_bw} = \log_2(\text{Sf}_{\text{high}}) - \log_2(\text{Sf}_{\text{low}}) \tag{4}$$

If the cell's response at the lowest spatial frequency measured (0.1 cycle deg^{-1}) was higher than half the best response, we defined it as a low-pass cell without a bandwidth.

Low spatial frequency suppression ratio (LSFS). LSFS is the ratio of a cell's response to the grating of lowest spatial frequency that was presented and the response to the grating of optimal spatial frequency:

$$\text{LSFS} = \frac{R(\text{Sf}_{\text{lowest}})}{R(\text{Sf}_{\text{optimal}})} \tag{5}$$

Low spatial frequency variance (LSFV). Based on the fitted curve, the left branch of the curve from 1/16 of the optimal spatial frequency to the optimal spatial frequency was used to calculate LSFV by the following equation:

$$\text{LSFV} = \frac{\int_{\text{Sf}_{\text{optimal}}/16}^{\text{Sf}_{\text{optimal}}} R(\text{Sf}) \times (\log_{16}(\text{Sf}) - \log_{16}(\text{Sf}_{\text{optimal}}))^2 \times d\log_{16}(\text{Sf})}{\int_{\text{Sf}_{\text{optimal}}/16}^{\text{Sf}_{\text{optimal}}} R(\text{Sf}) \times d\log_{16}(\text{Sf})} \tag{6}$$

To calculate LSFV we tried different low-spatial-frequency endpoints, from $\text{Sf}_{\text{optimal}}/2$ down to $\text{Sf}_{\text{optimal}}/30$. We found that the correlation between LSFV and LSFS increased when the denominator increased, and it reached an asymptotic value when the denominator was 16, approximately. So we used $\text{Sf}_{\text{optimal}}/16$ for the low frequency endpoint.

We categorized cells into simple and complex classes on the basis of the modulation ratio, $M = [R(F_1)/R(F_0)]$, where $R(F_1)$ is the fundamental response and $R(F_0)$ the DC response to drifting sine gratings. If the modulation ratio is greater than 1, we call the cell a simple cell; a complex cell has a modulation ratio smaller than 1 (but see Mechler & Ringach, 2002).

Results

Tuning functions for five representative neurones are shown in Fig. 2 illustrating the range of tuning of the population. There are a number of cells that are sharply tuned for spatial frequency and orientation (Fig. 2*G* and *H*). In the population of cells there is a spectrum of tuning (Fig. 2*A*–*F*) where the tuning for both measures covary. There are a few cells that are relatively sharply tuned for spatial frequency but poorly tuned for orientation (Fig. 2*I* and *J*). There were no cells with sharp orientation tuning that were low-pass in spatial frequency.

As described in the Introduction and Methods there are a number of ways of quantifying the tuning. The most familiar method is bandwidth. This captures the shape of the tuning curve locally, around the peak. Another measure, the orientation circular variance, estimates the global shape of the tuning curve. Previously, we have shown there is a correlation between local and global measures of tuning for orientation, with a correlation coefficient of 0.72 (Ringach *et al.* 2002*b*).

Here we report that there is also a strong correlation in the spatial frequency domain between a local measure, spatial frequency bandwidth, and a global measure, low spatial frequency variance (LSFV) (Fig. 3; $r = 0.74$, $n = 241$). Small values of low spatial frequency variance (0.1 or less) signify a sharp attenuation of the response from the peak to spatial frequencies 16 times less than the peak. Values of LSFV of between 0.25 and 0.3 indicate broad tuning. As shown in Fig. 1, cells with the same spatial frequency bandwidth can have different values of LSFV. In general, if the bandwidth is equal but the LSFV is lower, it means that the responses at the lowest spatial frequencies, particularly those below the half-maximum response, are more attenuated. This is analogous, we believe, to the different degrees of attenuation seen at off optimal and orthogonal orientations in cells with the same orientation bandwidth but different values of circular variance. As pointed out earlier, the high frequency limb of

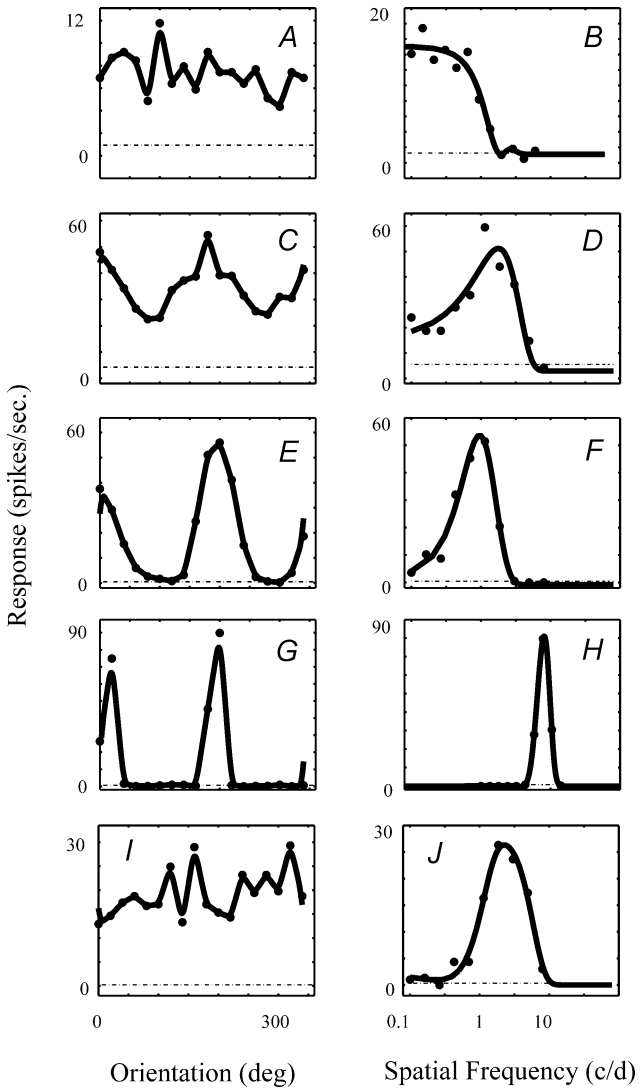

Figure 2. Individual tuning functions from five cells showing the range of tuning found among the V1 population
Each pair of graphs shows orientation tuning on the left and spatial frequency tuning on the right. The curve through the orientation data (left column) was smoothed with a Hanning window filter. The smooth curve drawn through the spatial frequency data was the best fitting difference of Gaussians function (see eqn (3)).

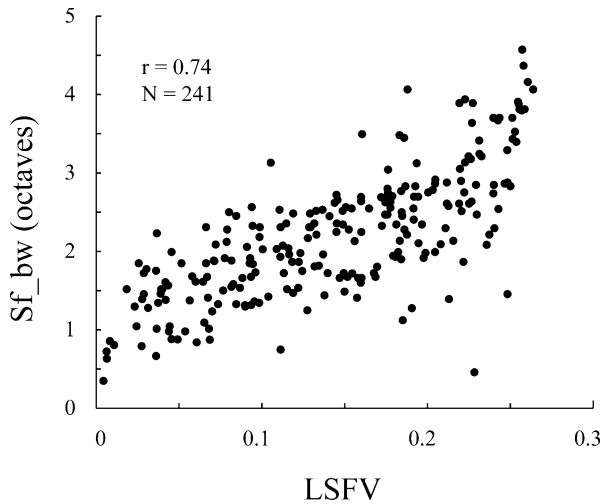

Figure 3. The correlation between the measure of global selectivity at low spatial frequencies, low spatial frequency variance (LSFV) and the measure of selectivity local to the peak, spatial frequency bandwidth (Sf_bw)
There is a strong correlation between these two measures, but it is not 1 : 1 or linear.

the spatial frequency tuning function is likely to be strongly influenced by the smallest subunit size of the receptive field and, as we will pursue in more depth in the discussion, is not as likely to be dependent on cortical suppression as is the low frequency limb of the tuning function. Spatial frequency bandwidth is partly dependent on degree of the high frequency attenuation, and this will not enter into the LSFV measure.

We compared the LSFV measure with a previously adopted 'global' measure of low spatial frequency attenuation, low spatial frequency suppression (LSFS; Ringach *et al.* 2002*a*). LSFS is obtained by dividing the response at the lowest spatial frequency by the response at the preferred spatial frequency. LSFV and LSFS are highly correlated ($r = 0.86$, $n = 306$). However the LSFS index shows a floor effect, whereas the LSFV has a greater dynamic range (Fig. 4). LSFV uses all the data from the peak to the lowest frequency whereas LSFS uses only two points. Consequently, the LSFV measure provides a more comprehensive measure of the low frequency limb of the tuning function and we chose to use this as the global measure of spatial frequency selectivity.

Comparison between local and global measures of orientation and spatial frequency

The main question we addressed in this study was whether, and how much, global measures of tuning for orientation and spatial frequency were correlated when stimulation was steady-state. This comparison is shown in Fig. 5. There is a strong correlation between orientation circular variance (Ori_CV) and LSFV ($r = 0.77$, $n = 306$). Thus, cells that are weakly suppressed or not suppressed at (or near) the orthogonal-to-preferred orientation also tend to have much less attenuation over the range of spatial frequencies below the peak and cells that are highly suppressed at the orthogonal orientation tend to be highly suppressed at spatial frequencies below the peak.

There are some exceptions to the main trend. Notably there are a small number of cells that are unselective for orientation, but that are tuned for spatial frequency. Such neurones show strong low spatial frequency attenuation (see cells plotted in the upper left quadrant of Fig. 5).

The result in Fig. 5 can be compared to the correlation between orientation bandwidth and spatial frequency bandwidth (Fig. 6) where the correlation is considerably weaker ($r = 0.46$, $n = 241$). The results on bandwidth correlation are similar to those reported in a previous study (DeValois *et al.* 1982). We also compared Ori_bw and LSFV; there is not a strong correlation between them ($r = 0.51$, $n = 241$). In addition we analysed the relationship between Ori_CV and LSFS; there is a strong correlation between them ($r = 0.69, n = 308$). It is also worth noting that there was only a very weak correlation between spatial frequency preference and LSFV ($r = -0.40, n = 308$); neurones that preferred low spatial frequency could be as selective for spatial frequency as those that preferred high.

About 80% of cells (241/306) have a measurable bandwidth in both spatial frequency and orientation. But there

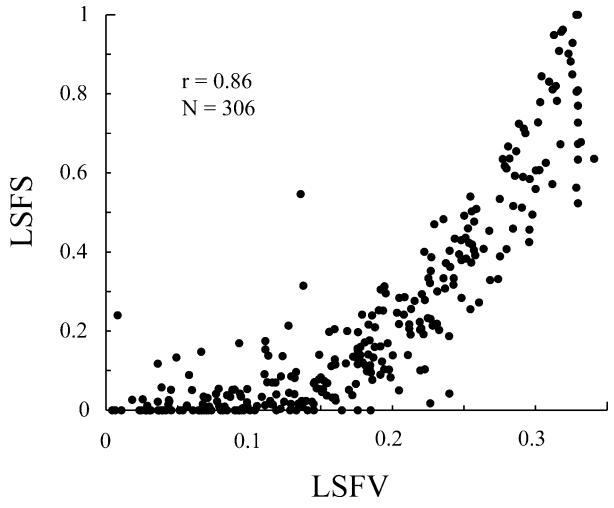

Figure 4. A comparison between two measures of low spatial frequency attenuation
Plotted on the *x*-axis is our new measure, low spatial frequency variance (LSFV, eqn (6)), while low spatial frequency suppression (LSFS, eqn (5)) is plotted on the *y*-axis. There is clear compression of the LSFS measure at low values whereas LSFV offers more dynamic range for sharply attenuated cells.

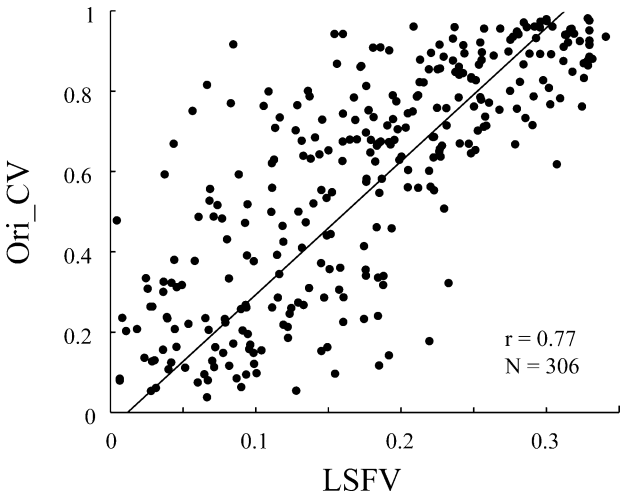

Figure 5. A comparison between global measures of selectivity
Orientation circular variance (Ori_CV) and low spatial frequency selectivity (LSFV) are strongly correlated ($r = 0.77$, $n = 306$) for the V1 population sample.

is a small population, 20% of V1 cells, so broadly tuned that their response does not drop below half the maximum at low spatial frequency or on either side of the preferred orientation. This is not a function of cortical layer. Not all the untuned cells are in layer 4, but rather they are ubiquitous in V1: cells poorly tuned for spatial frequency are found throughout all cortical layers, as was shown previously for orientation (as measured by Ori_CV; Ringach *et al.* 2002*b*).

Spontaneous rate and response at low spatial frequency

In a previous study on orientation selectivity we plotted the response at the orthogonal orientation against the spontaneous rate of the neurone (Ringach *et al.* 2002*b*). We found a strong trend: cells that were most orientation selective had a suppression of the response below the spontaneous rate at the non-preferred orientation. In Fig. 7 we have plotted on the *x*-axis the response to the lowest spatial frequency tested (usually about 0.1 cycle deg^{-1}) against the spontaneous discharge of the neurone (on the *y*-axis). The size of the symbol representing each cell shows the low spatial frequency variance, LSFV. Large sized symbols represent low values of LSFV, meaning strong attenuation at spatial frequencies below the peak of the tuning curve. Small symbols indicate cells with large values of LSFV which indicate weak attenuation at low spatial frequencies. Cells with values of spontaneous firing rate less than 0.1 spike s^{-1} are plotted at the origin or on the *x*-axis. Cells with responses less than 0.1 spike s^{-1} in response to the lowest spatial frequency tested are plotted at the origin or on the *y*-axis. It can be seen that there are some cells clustered along the *y*-axis (20/306) and these are generally cells with low values of LSFV meaning they are very selective for spatial frequency. However, most data points are below the diagonal line that signifies equality between low spatial frequency response and spontaneous firing rate. A point below the diagonal line means that the cell's firing rate at low spatial frequency is higher than its spontaneous rate. This is different from what we see in the orientation domain (Ringach *et al.* 2002*b*). But we can still see that some cells produce responses to low spatial frequency that are lower than the spontaneous firing rate.

Figure 8 illustrates the covariation of spontaneous firing rate and LSFV, and spontaneous firing rate and Ori_CV. Both scatter plots in Fig. 8 suggest that a cell with strong attenuation of its responses to non-optimal stimuli (and therefore low LSFV and low Ori_CV) also tends to have a lower spontaneous firing rate.

Simple and complex cells

We can split the cells into two groups based on their modulation ratio (F_1/F_0 ratio). If the F_1/F_0 ratio is greater than 1 we have called the cell a simple cell; cells with F_1/F_0 ratios less than 1 are called complex (Skottun *et al.* 1991). When we consider global measures

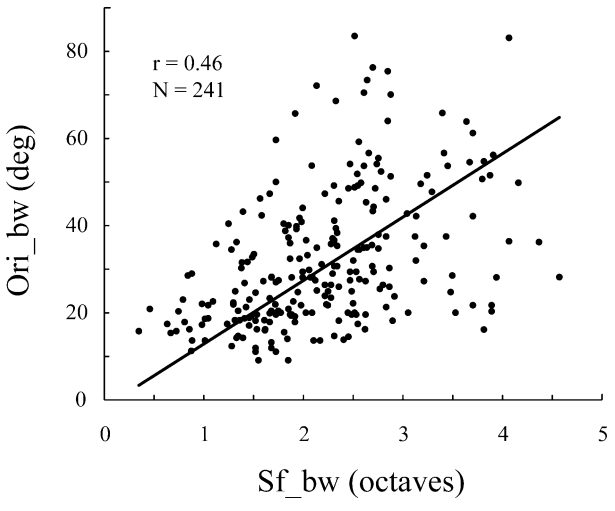

Figure 6. A comparison between local measures of selectivity
Orientation bandwidth (Ori_bw), and spatial frequency bandwidth (Sf_bw) are weakly correlated ($r = 0.46$, $n = 241$) for the V1 population sample. This result is very similar to that reported by DeValois *et al.* (1982).

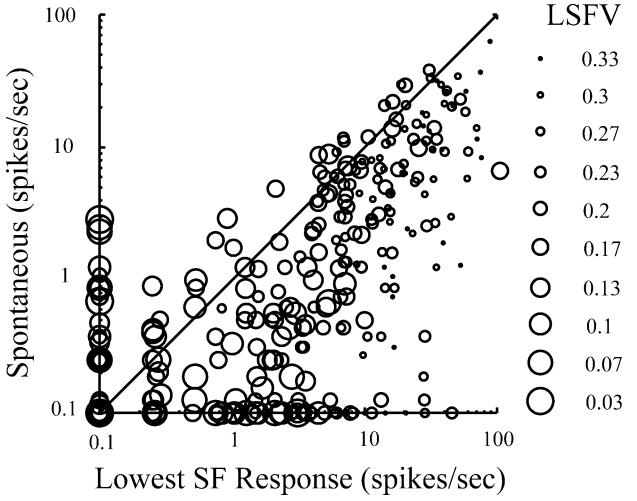

Figure 7. The response to the lowest spatial frequency tested (*x*-axis) is plotted against the spontaneous discharge rate of the cell (*y*-axis)
The size of the symbol shows the LSFV. Large symbols represent small LSFV values which indicate strong spatial frequency attenuation below the peak of the tuning curve. A small symbol size represents a large value of LSFV indicating weak spatial frequency attenuation.

of tuning within the population of cells classified as simple cells, there is quite a strong correlation between Ori_CV and LSFV ($r = 0.84$, $n = 127$). The correlation between (orientation and spatial frequency) bandwidths of simple cells is much less ($r = 0.41$, $n = 102$; Fig. 9*B*). It is likely that the apparent clustering in Fig. 9*A* may be due to the thresholding mechanism described recently by Mechler & Ringach (2002).

There is also a relatively strong correlation between Ori_CV and LSFV ($r = 0.68$, $n = 179$; Fig. 10*A*) for complex cells. However, a somewhat different pattern is seen among the complex cell population from the simple cell population. For the global measures there are few complex cells with low Ori_CV and low LSFV, suggesting that the most highly selective cells are in the simple cell group. So although there is a strong correlation between Ori_CV and LSFV, many of the complex cells are in the region (upper right quadrant of Fig. 10*A*) indicating poorer global selectivity. In comparison, the correlation for complex cells between the local measures, orientation and spatial frequency bandwidth, is relatively weak ($r = 0.43$, $n = 139$; Fig. 10*B*) and similar to that for the simple cell population.

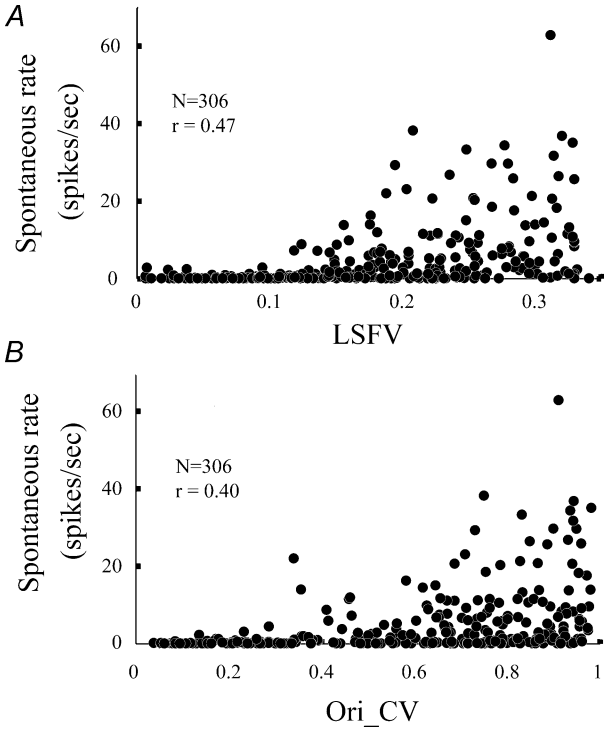

Figure 8. Scatter plots of cells' LSFV or Ori_CV and cells' spontaneous firing rate
A, the LSFV (*x*-axis) is plotted against the spontaneous discharge rate of the cell (*y*-axis). *B*, the Ori_CV (*x*-axis) is plotted against the spontaneous discharge rate of the cell (*y*-axis).

Discussion

In a recent series of experiments using dynamically flashed gratings we found that there was a strong correlation in the dynamic responses of V1 neurones between selectivity for orientation and spatial frequency (Ringach *et al.* 2002*a*; Bredfeldt & Ringach, 2002). Furthermore, a major result of the dynamics experiments is that suppression of non-optimal responses is very highly correlated with global measures of selectivity, for both orientation and spatial frequency. This result implies that the neuronal processes in the visual cortex that cause suppression of

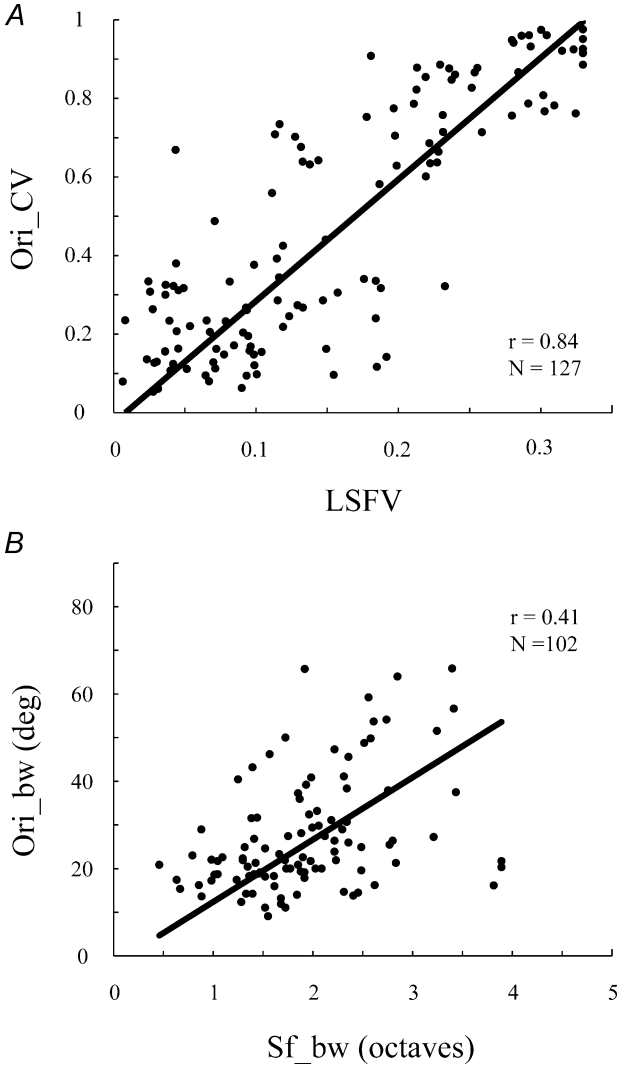

Figure 9. A comparison of the correlation between global and local selectivity measures of orientation and spatial frequency for simple cells
A shows that there is a strong correlation between Ori_CV and LSFV ($r = 0.84$, $n = 127$). *B* shows that there is a weak correlation between orientation bandwidth and spatial frequency bandwidth ($r = 0.41$, $n = 102$).

non-optimal responses are involved in establishing the global selectivities for orientation and spatial frequency in the cortical cells' responses to dynamical stimuli. In the present study we have extended this result to steady-state responses to drifting gratings, making use of the large natural diversity in steady-state orientation and spatial frequency tuning. Therefore, both dynamical and steady-state experiments are consistent in indicating the important role of intra-cortical interactions in causing visual spatial selectivity.

In this study we introduced a new measure to assess the degree of low spatial frequency attenuation – the low spatial frequency variance or LSFV. Using this new global measure for low spatial frequency selectivity and a corresponding global measure of orientation selectivity, circular variance, we found a strong correlation between orientation and spatial frequency selectivity during steady-state stimulation with drifting sinewave gratings (Fig. 5). This held for both simple (Fig. 9) and complex (Fig. 10) cell groups; the correlation for simple cells was the strongest. Previous research had established a weaker positive correlation between local measures of steady-state orientation and spatial frequency tuning, the orientation and spatial frequency bandwidths (DeValois *et al.* 1982), and we replicated this result. We need to consider why the global measures of selectivity are so highly correlated, and why the local measures are so much less correlated.

The correlation between global measures

Orientation selectivity has been well characterized in previous studies of monkey V1 (Schiller *et al.* 1976; DeValois *et al.* 1982; Parker & Hawken, 1988; Leventhal *et al.* 1995; Ringach *et al.* 2002*b*). The global measure of orientation selectivity that we used in this study is similar to other global measures of orientation selectivity used in other studies (Mardia, 1972; Batschelet, 1981; Swindale, 1998; Zhou *et al.* 2000). As we have reported recently (Ringach *et al.* 2002*b*), there is good agreement among investigators that there is a broad range of orientation selectivity across the population of V1 neurones as estimated by these global measures.

In this paper we establish for the first time that there is a similar broad distribution of global measures of steady-state selectivity for spatial frequency as evidenced by the scatter plots in Figs 4 and 5.

In order to understand why orientation circular variance and LSFV are so highly correlated we need to consider the contributions of different processes to the selectivity for orientation and spatial frequency in monkey striate cortex. Based on the results from studies of the responses to dynamical stimuli, we have proposed (Ringach *et al.* 1997; Bredfeldt & Ringach, 2002, 2003; Shapley *et al.* 2003) that there are different components involved in the generation of the spatial selectivities of the V1 neurones. The first component is set up by feedforward mechanisms from LGN afferents that provide excitatory input to V1. By itself this LGN input provides broad tuning around the peak for orientation and modest selectivity for spatial frequency. A second, intracortical component, provides additional suppression at all orientations and at spatial frequencies from the peak of the tuning curve down to zero spatial frequency. This suppression (which is probably implemented by intracortical inhibition) leads

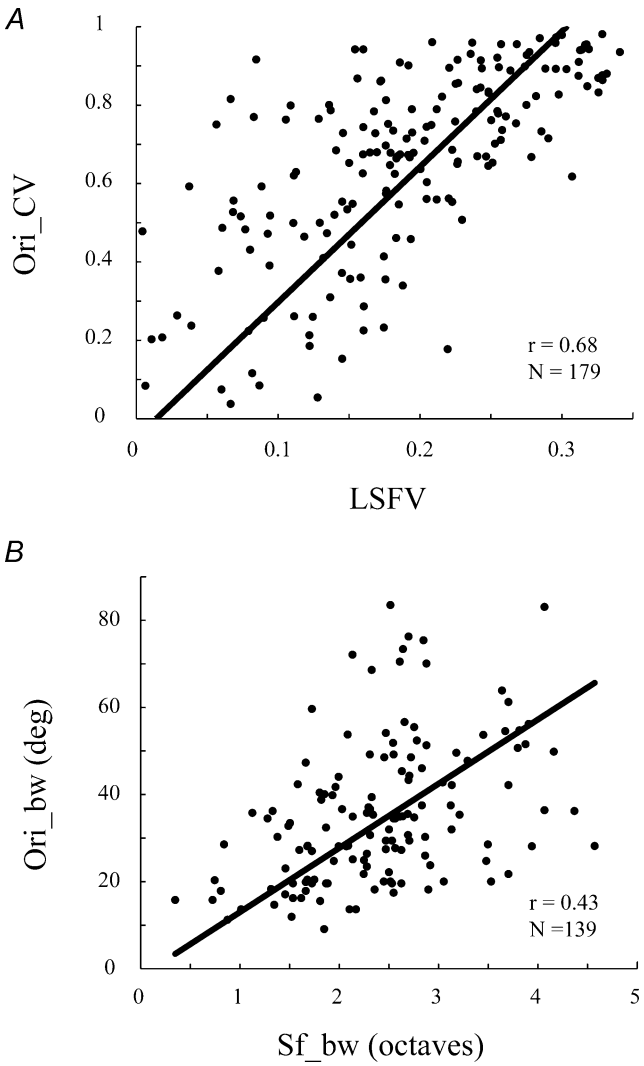

Figure 10. A comparison of the correlation between global and local selectivity measures of orientation and spatial frequency for complex cells

A shows that there is a moderate correlation between Ori_CV and LSFV ($r = 0.68$, $n = 179$). *B* shows that there is a weak correlation between orientation bandwidth and spatial frequency bandwidth ($r = 0.43$, $n = 139$).

to enhanced spatial selectivity that is captured by the two measures of global selectivity that we used: Ori_CV for orientation and LSFV for the low spatial frequency limb of the spatial frequency tuning curve.

The most selective cells in V1 are simple cells (Fig. 9*A*). The most recent models of V1 networks suggest that simple cells receive strong intracortical inhibition that should be observable as strong global suppression in the steady-state tuning of cells (Troyer *et al.* 1998; McLaughlin *et al.* 2000; Shelley *et al.* 2002; Miller, 2003). Therefore, the strong correlation we found between global measures of selectivity for orientation and spatial frequency is consistent with the proposal that there is an important role of intracortical suppression (likely to be mediated by cortical inhibition) in orientation and spatial frequency selectivity (Ringach *et al.* 2002*a*; Bredfeldt & Ringach, 2002; Shapley *et al.* 2003).

Another feature of the data shown here is that there is considerable scatter in the relationship between orientation and spatial frequency selectivity. As yet we do not have theories that model cells in all the different cortical layers. Most explicit models concentrate on the input layers (Troyer *et al.* 1998; McLaughlin *et al.* 2000; Shelley *et al.* 2002; Miller, 2003) yet our results are from all cortical layers. Further refinements of models to other cortical layers and cell classes will need to predict the diversity in the interrelationship between spatial frequency and orientation selectivity that we have shown in this study for steady-state stimulation.

The weaker correlation between local measures

It is more complicated to account for the weaker correlation between the local measures, orientation and spatial frequency bandwidths. This is because the factors that control bandwidths for orientation and spatial frequency are less well understood. However, given the following review of what is known, it seems plausible that the correlation should exist, and should be weaker than the global correlations. Many V1 cells are selective for spatial frequency. For many of these cells we expect that the response attenuation beyond the peak, on the high frequency limb of the spatial frequency tuning curve, is due to the spatial frequency resolution of the smallest subunit of the V1 receptive field. It is not known for certain, but widely believed that the size of the receptive field subunits is determined by the pattern of feedforward inputs from the LGN (Parker & Hawken, 1988). There is no clear connection between receptive field subunit size and orientation selectivity. Therefore, the variation in spatial frequency bandwidth caused by variation in receptive field subunit size should have little or no correlation with orientation bandwidth (or Ori_CV).

The processes that determine the shape of the low spatial frequency limb of the spatial frequency tuning curve probably affect both spatial frequency bandwidth and LSFV, and these could cause the weak correlation that does exist with orientation selectivity. Low spatial frequency tuning is probably due to a combination of feedforward input from the LGN, which can provide a very small amount of low spatial frequency attenuation, and intracortical suppressive mechanisms that provide the main contribution to sharply tuned cells. Recently, it has been suggested that synaptic depression of the thalamocortical synapses could also provide a globally untuned suppression signal (Freeman *et al.* 2002; Carandini *et al.* 2002). The factors that determine orientation bandwidth are also not well understood. Certainly the pattern of feedforward input that is inferred to come from the LGN must play an important role (Reid & Alonso, 1995; Ferster *et al.* 1996). However, the strength of tonic inhibition, untuned for orientation, can also play a role in reducing the orientation bandwidth by keeping the firing rate low at off-peak orientations (Troyer *et al.* 1998; Carandini & Ferster, 2000). From recent results from our group on orientation dynamics, there also may be suppression tuned for orientation in the most highly tuned V1 neurones (Ringach *et al.* 2003), and this tuned suppression could also contribute to narrowing the orientation bandwidth. Therefore, while similar neuronal processes may shape low spatial frequency tuning and orientation bandwidth, causing some correlation between the bandwidth measures, the likely independence of the processes that control high spatial frequency tuning would cause decorrelation between spatial frequency bandwidth and measures of orientation selectivity. It is not surprising then that there is much less correlation between the orientation and spatial frequency bandwidths than between Ori_CV and LSFV.

References

Adorjan P, Levitt JB, Lund JS & Obermayer K (1999). A model for the intracortical origin of orientation preference and tuning in macaque striate cortex. *Vis Neurosci* **16**, 303–318.

Batschelet E (1981). *Circular Statistics in Biology*. Academic Press, London.

Ben-Yishai R, Bar-Or RL & Sompolinsky H (1995). Theory of orientation tuning in visual cortex. *Proc Natl Acad Sci U S A* **92**, 3844–3848.

Bredfeldt CE & Ringach DL (2002). Dynamics of spatial frequency tuning in macaque V1. *J Neurosci* **22**, 1976–1984.

Bruno RM & Simons DJ (2002). Feedforward mechanisms of excitatory and inhibitory cortical receptive fields. *J Neurosci* **22**, 10966–10975.

Campbell FW, Cooper GF & Enroth-Cugell C (1969). The spatial selectivity of the visual cells of the cat. *J Physiol* **203**, 223–235.

Carandini M & Ferster D (2000). Membrane potential and firing rate in cat primary visual cortex. *J Neurosci* **20**, 470–484.

Carandini M, Heeger DJ & Senn W (2002). A synaptic explanation of suppression in visual cortex. *J Neurosci* **22**, 10053–10065.

DeValois RL, Albrecht DG & Thorell LG (1982). Spatial frequency selectivity of cells in macaque visual cortex. *Vis Res* **22**, 545–549.

Enroth-Cugell C & Robson JG (1966). The contrast sensitivity of retinal ganglion cells of the cat. *J Physiol* **187**, 517–552.

Ferster D, Chung S & Wheat H (1996). Orientation selectivity of thalamic input to simple cells of cat visual cortex. *Nature* **380**, 249–252.

Freeman TCB, Durand S, Kiper DC & Carandini M (2002). Suppression without inhibition in visual cortex. *Neuron* **35**, 759–771.

Hawken MJ, Shapley RM & Grosof D (1996). Temporal-frequency selectivity in monkey visual cortex. *Vis Neurosci* **13**, 477–492.

Kuffler SK (1953). Discharge patterns and functional organization of mammalian retina. *J Neurophysiol* **16**, 37–68.

Leventhal AG, Thompson KG, Liu D, Zhou Y & Ault SJ (1995). Concomitant sensitivity to orientation, direction, and color of cells in layers 2, 3, and 4 of monkey striate cortex. *J Neurosci* **15**, 1808–1818.

Mardia KV (1972). *Statistics of Directional Data*. Academic Press, London.

McLaughlin D, Shapley R, Shelley M & Wielaard J (2000). A neuronal network model of sharpening and dynamics of orientation tuning in an input layer of macaque primary visual cortex. *Proc Natl Acad Sci U S A* **97**, 8087–8092.

Mechler F & Ringach DL (2002). On the classification of simple and complex cells. *Vision Res* **42**, 1017–1033.

Miller KD (2003). Understanding layer 4 of the cortical circuit: a model based on cat V1. *Cereb Cortex* **13**, 73–82.

Movshon JA, Thompson ID & Tolhurst DJ (1978). Spatial and temporal contrast sensitivity of neurons in areas 17 and 18 of the cat's visual cortex. *J Physiol* **283**, 101–120.

Nelson S, Toth L, Sheth B & Sur M (1994). Orientation selectivity of cortical neurons during intracellular blockade of inhibition. *Science* **265**, 774–777.

Parker AJ & Hawken MJ (1988). Two-dimensional spatial structure of receptive fields in monkey striate cortex. *J Opt Soc Am A* **5**, 598–605.

Reid RC & Alonso JM (1995). Specificity of monosynaptic connections from thalamus to visual cortex. *Nature* **378**, 281–284.

Ringach DL, Bredfeldt CE, Shapley RM & Hawken MJ (2002*a*). Suppression of neural responses to nonoptimal stimuli correlates with tuning selectivity in macaque V1. *J Neurophysiol* **87**, 1018–1027.

Ringach DL, Hawken MJ & Shapley R (1997). Dynamics of orientation tuning in macaque primary visual cortex. *Nature* **387**, 281–284.

Ringach DL, Hawken MJ & Shapley R (2003). Dynamics of orientation tuning in macaque V1: the role of global and tuned suppression. *J Neurophysiol* **90**, 342–352.

Ringach DL, Shapley RM & Hawken MJ (2002*b*). Orientation selectivity in macaque V1: diversity and laminar dependence. *J Neurosci* **22**, 5639–5651.

Sceniak MP, Hawken MJ & Shapley R (2001). Visual spatial characterization of macaque V1 neurons. *J Neurophysiol* **85**, 1873–1887.

Schiller PH, Finlay BL & Volman SF (1976). Quantitative studies of single-cell properties in monkey striate cortex. II. Orientation specificity and ocular dominance. *J Neurophysiol* **39**, 1320–1333.

Shapley R, Hawken MJ & Ringach DL (2003). Dynamics of orientation selectivity in the primary visual cortex and the importance of cortical inhibition. *Neuron* **38**, 689–699.

Shelley M, McLaughlin D, Shapley R & Wielaard J (2002). States of high conductance in a large-scale model of the visual cortex. *J Comput Neurosci* **13**, 93–109.

Skottun BC, DeValois RL, Grosof DH, Movshon JA, Albrecht DG & Bonds AB (1991). Classifying simple and complex cells on the basis of response modulation. *Vis Res* **31**, 1079–1086.

Somers DC, Nelson SB & Sur M (1995). An emergent model of orientation selectivity in cat visual cortical simple cells. *J Neurosci* **15**, 5448–5465.

Swindale NV (1998). Orientation tuning curves: empirical description and estimation of parameters. *Biol Cybern* **78**, 45–56.

Troyer TW, Krukowski AE, Priebe NJ & Miller KD (1998). Contrast-invariant orientation tuning in cat visual cortex: thalamocortical input tuning and correlation-based intracortical connectivity. *J Neurosci* **18**, 5908–5927.

Zhou H, Friedman HS & von der Heydt R (2000). Coding of border ownership in monkey visual cortex. *J Neurosci* **20**, 6594–6611.

Acknowledgements

This work was supported by NIH grants EY08300, EY01472, core grant P031-13079, NIH EY-12816 and Research to Prevent Blindness grant to the Jules Stein Eye Institute, UCLA. Thanks go to Elizabeth Johnson, J. Andrew Henrie, and Patrick Williams for help with experiments and Kukjin Kang for helpful discussion.